Front. Optoelectron. 2016, 9(3): 483–488
DOI 10.1007/s12200-016-0559-6

RESEARCH ARTICLE

Application of SOI microring coupling modulation in microwave photonic phase shifters

Rui YANG, Linjie ZHOU (✉), Minjuan WANG, Haike ZHU, Jianping CHEN

State Key Laboratory of Advanced Optical Communication Systems and Networks, Department of Electronic Engineering, Shanghai Jiao Tong University, Shanghai 200240, China

Abstract Phase shifter is one of the key devices in microwave photonics. We report a silicon microring resonator with coupling modulation to realize microwave phase shift. With coupling tuning of the Mach-Zehnder interferometer (MZI) coupler to change the resonator from under-coupling to over-coupling, the device can realize a π phase shift on the incoming microwave signal with a frequency up to 25 GHz. The device can also realize 2.5π continuous phase tuning by manipulating the three DC bias voltages applied on the MZI coupler.

Keywords ring resonator, phase shifter, microwave photonics

1 Introduction

Microwave photonics has received continuous attention for its capability in radio frequency (RF) signal processing. Microwave photonic phase shifter is one of the key elements, which could be applied in phased array radars and microwave filters [1]. In traditional schemes, one can use distributed feedback (DFB) lasers [2], stimulated Brillouin scattering (SBS) [3] and slow- and fast-light effects in semiconductor optical amplifiers (SOAs) [4] to realize microwave photonic phase shift. The integrated devices like $LiNbO_3$ Mach-Zehnder interferometers (MZIs) are also applicable in practical use [5]. In recent years, silicon-on-insulator (SOI) microwave photonic phase shifters have drew more and more attention due to their small footprint, large bandwidth and low power consumption. Nowadays, SOI microrings are regarded as one of the ideal structures for phase shifters. Microrings have continuously variable phase change around resonances which could be used for phase shift. It is required to broaden the continuous tunable range of phase shift while simultaneously reduce the amplitude variation in many applications. In Ref. [6], the authors adopted the thermo-optical effect in a SOI mircoring to achieve a $0-1.46\pi$ phase tuning range for a 40 GHz RF signal. In Ref. [7], the authors achieved 3.3π continuous phase shift by cascading two electrically controlled microrings.

Compared to the traditional microring resonator with direct cavity modulation, the microring resonator with coupling modulation has the advantage of a large bandwidth beyond the cavity linewidth limitation [8]. The coupling modulation is usually realized in a MZI coupler. Both on-off keying (OOK) and binary phase-shift keying (BPSK) optical modulations can be generated by such a device [9]. It is noticed that when the MZI coupler is driven by a push-pull RF signal at its critical coupling point, the output phase will experience a π phase shift. This is why this structure can achieve a chirp-free BPSK modulation. In this paper, we used the coupling-modulated ring resonator to achieve phase shift for RF signals. A maximum of 2.5π continuous phase change is obtained by changing the voltages applied on the two arms of the MZI coupler.

2 Phase shift principles and simulations

Figure 1 depicts the schematic of the device. Intuitively,\ the structure can be regarded as a combination of a MZI and a microring resonator. The MZI is composed of two 2×2 3-dB multimode interferometers (MMIs). The two arms of the MZI have a length difference of 14.6 μm. One output port of the right MMI is connected back to one input port of the left MMI to form a resonance loop. Two back-to-back series connected pn junctions are positioned in the MZI arms with an active waveguide length of 800 μm. We use three bias voltages V_{up}, V_{down}, and V_b to tune the refractive indices of the upper and lower arms of the MZI

Received November 16, 2015; accepted December 21, 2015

E-mail: ljzhou@sjtu.edu.cn

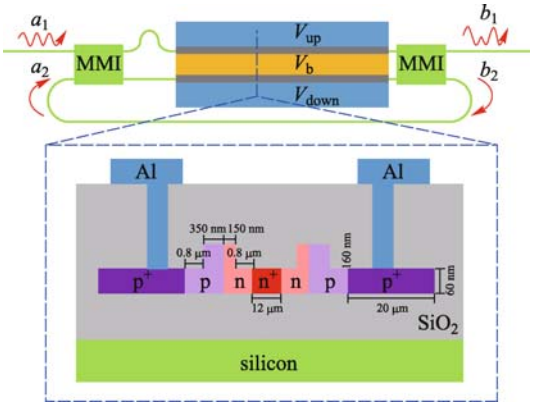

Fig. 1 Schematic of a microring resonator with coupling enabled by an asymmetric MZI coupler. The blue regions outside the MZI arms are the p-doped regions, and the yellow region in between the MZI arms is the n-doped region. Inset: cross-sectional view of the MZI modulation arms

to get a desired output phase change.

The inset depicts the cross section of the active arms. The silicon waveguide is 500 nm wide and 220 nm high with a slab thickness of 60 nm. Carrier depletion in the silicon pn junctions is utilized to modulate the optical phase. Taking into account that holes have a higher refractive index modulation efficiency than electrons, the pn junction was designed to have a lateral offset of 100 nm toward the n region side from the ridge waveguide center. Consequently, the width of the p/n region is 350 nm/150 nm. The wider p region also reduces the optical loss due to the smaller absorption coefficient of holes [10]. Two p^+ regions are both 20 μm in width. In the center, the n^+ region has a width of 12 μm.

We first use the transfer matrix method [11] to study the behavior of the device. The output transfer function is given by

$$\frac{b_1}{a_1} = \frac{\alpha(t^2+\kappa^2) + te^{i\theta}}{\alpha t + e^{i\theta}}, \tag{1}$$

where α and θ are the light field amplitude transmission and phase shift of the feedback ring waveguide, respectively, t and κ are the through and cross transmission coefficients of the MZI coupler, respectively, given by

$$t = \frac{1}{2}[\alpha_{up}e^{-i(\varphi_0+\Delta\varphi_{up})} - \alpha_{down}e^{-i\Delta\varphi_{down}}], \tag{2}$$

$$\kappa = -\frac{i}{2}[\alpha_{up}e^{-i(\varphi_0+\Delta\varphi_{up})} + \alpha_{down}e^{-i\Delta\varphi_{down}}], \tag{3}$$

where α_{up} and α_{down} are the light field amplitude transmission through the MZI two arms, φ_0 is the initial phase due to the length difference of the two arms, $\Delta\varphi_{up}$ and $\Delta\varphi_{down}$ are the phase changes induced by the applied voltages.

From Eqs. (1)–(3), we can get the amplitude and phase responses of the device under various DC biases on the electrodes. The output phase shift relative to that without biases is

$$\Delta\Phi = \text{angle}\left(\frac{b_1'}{b_1}\right), \tag{4}$$

where b_1 and b_1' are the output transmitted fields before and after bias tuning. If the device is driven in a push-pull fashion, i.e., $V_b - V_{up} = -(V_b - V_{down})$, and operated at the critical-coupling point, the output phases are always π phase different.

In our simulation, the effective index of the undoped silicon waveguides is chosen as 2.515 according to the mode calculation. The waveguide loss is assumed to be 2.53 dB/cm. For the active waveguide, its effective index and loss are dependent on the voltage applied on the pn junction. According to our previous measurements, we adopt the following empirical formulas for the effective index change and the waveguide propagation loss change:

$$n_{eff} = -1.5 \times 10^{-5} V_{pn}, \tag{5}$$

$$\Delta\text{loss(dB/cm)} = 20.23 + 0.34V_{pn}, \tag{6}$$

where V_{pn} ($= V_{up} - V_b$ or $V_{down} - V_b$) is the voltage on the pn junction.

Figure 2 shows the typical resonance spectra when the mirroring works in the over-coupling and under-coupling regimes. They have an equal resonance extinction ratio but distinct phase responses. From the phase difference curve, we see that an exact π phase shift occurs at the resonance wavelength.

Apart from the strict π phase shift, our device could also provide a large-range continuous phase shift by manipulating the three bias voltages. Figure 3 shows the output

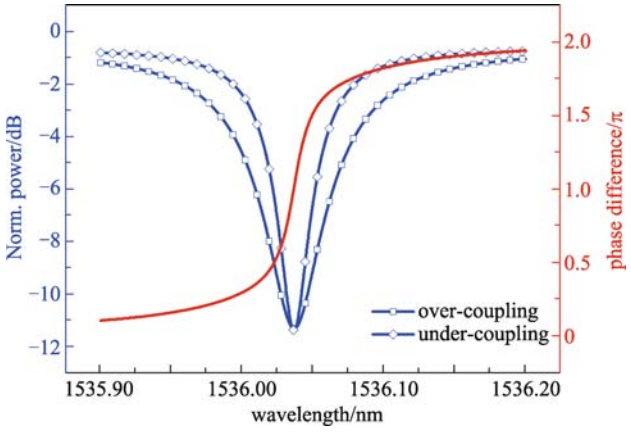

Fig. 2 Optical output power and phase difference responses of the device working at over-coupling and under-coupling

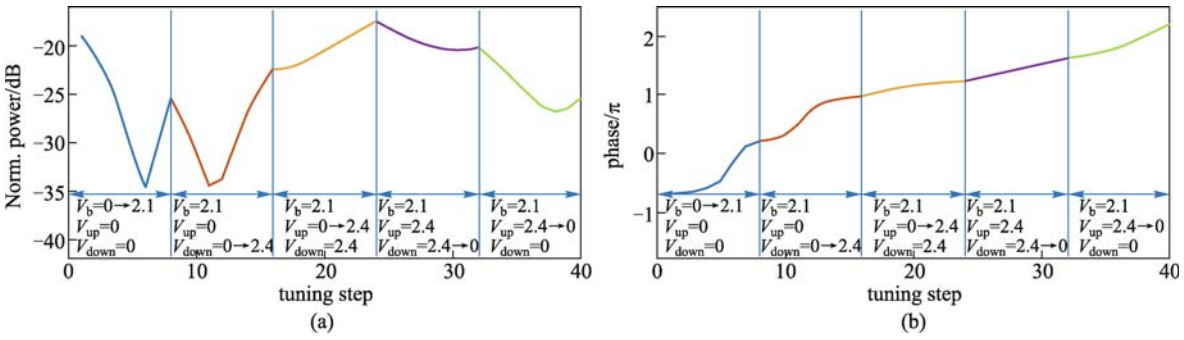

Fig. 3 Simulated device performances for (a) optical power and (b) optical phase responses upon bias tuning. The bias voltages in each tuning zone are labeled on the graphs

power and phase responses when we change the three bias voltages. The input wavelength is slightly detuned from the critical coupling wavelength. A large phase shift of nearly 2.5π is achievable. The voltage tuning is divided into five zones.

1) V_{up} and V_{down} are set to 0 V, and V_b varies from 0 to 2.1 V. As seen from Figs. 4(a) and 4(b), this will make the resonance red-shift a little bit due to the depletion of free-carriers in the pn junctions. As the result, the phase increases and a rapid change is observed when the resonance is shifted to the operation wavelength.

2) V_b and V_{up} remain at 2.1 and 0 V, respectively, while V_{down} is changed from 0 to 2.4 V. As the decreasing reverse bias of the lower arm, the resonance wavelength is blue-shifted. It can also be noticed from Figs. 4(c) and 4(d) that coupling changes from under-coupling to over-coupling, resulting in a further increased phase.

3) V_b and V_{down} remain at 2.1 and 2.4 V, respectively, while V_{up} is tuned from 0 to 2.4 V. The coupling changes from over-coupling to under-coupling as shown in Figs. 4 (e) and 4(f). The phase at the operation wavelength continues to grow.

4) V_b and V_{up} remain at 2.1 and 2.4 V, respectively, while V_{down} drops down from 2.4 to 0 V. As the reverse bias on the MZI lower arm increases, the resonance experiences a red-shift and goes into deep under-coupling as shown in Figs. 4(g) and 4(h), leading to the rise of output phase.

5) V_b and V_{down} remain at 2.1 and 0 V, respectively, while V_{up} reduces from 2.4 to 0 V. The reverse bias on the MZI top arm increases, making the resonance red-shift and coupling toward critical coupling as shown in Figs. 4(i) and 4(j). The transmission spectra return to the end stage of zone 1) after a 2π phase shift.

The above phase shift is achieved near resonance wavelength, and therefore phase change is always accompanied by a variation in output power. A variable optical attenuator could be used after the device to adjust the output optical power.

3 Device structure and fabrication

Figure 5 shows the top-view microscope image of the fabricated Mach-Zehnder racetrack resonator with a tunable MZI coupler. The aluminum lines in the traveling-wave electrode (TWE) are 10 μm wide and 800 μm long with a thickness of 0.75 μm. The gap size between the signal and the ground metal lines is 18 μm. The bending radius of the racetrack is 20 μm. Light is vertically coupled into and out of the chip through grating couplers with an insertion loss of 5 dB per facet.

Device fabrication was performed using A*Star's Institute of Microelectronics (IME) complementary metal-oxide-semiconductor (CMOS) compatible processes on a SOI wafer with a top silicon layer thickness of 220 nm and a buried oxide layer thickness of 2 μm. The device patterns were defined using 248-nm deep ultraviolet (DUV) photolithography and plasma dry etch. The etch depth is ~160 nm with a 60 nm slab remained. Ion implantation was used for doping. The doping concentrations of the lightly doped p and n regions are ~4×10^{17} cm^{-3} and ~1×10^{18} cm^{-3}, respectively. The doping concentrations of the heavily doped p^+ and n^+ regions are both ~10^{20} cm^{-3} for good ohmic contact. A 2.3 μm thick silicon dioxide layer was deposited using plasma-enhanced chemical vapor deposition (PECVD) followed by etch of contact holes. Finally, aluminum layer was sputtered and patterned to form metal connections.

4 Experiments and results

Figure 6 is the experimental setup to measure the RF signal phase shift. The red arrows represent the light signal paths, and the blue arrows represent the electric signal paths. Continuous-wave light from a tunable laser goes through a polarization controller (PC1) and is then modulated by a 20-GHz commercial $LiNbO_3$ Mach-Zehnder modulator

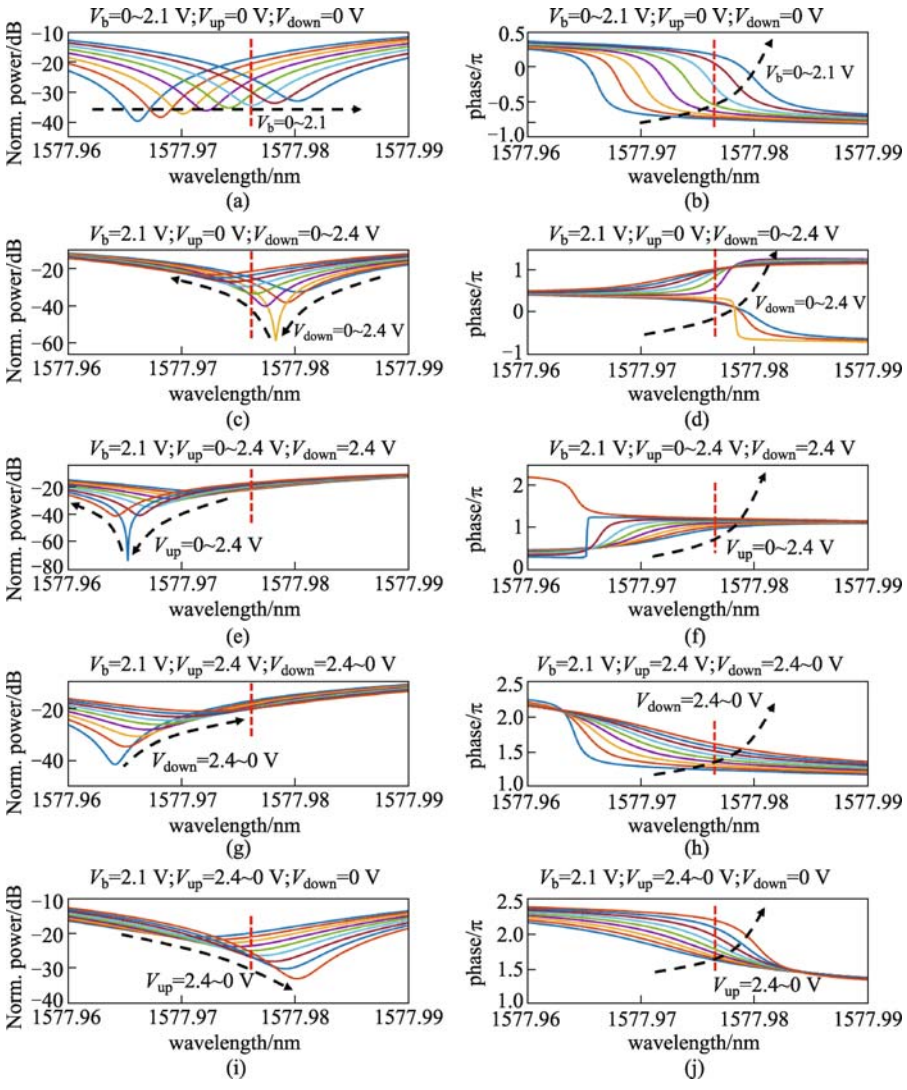

Fig. 4 Simulated optical power (left column) and phase (right column) transmission spectra of all tuning zones. The red dashed line denotes the operation wavelength. The black arrow indicates the spectrum evolution direction

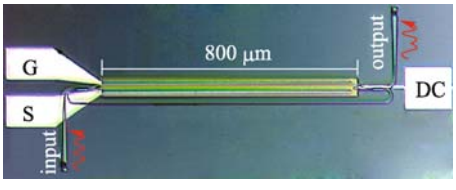

Fig. 5 Optical microscope image of the fabricated device. The total length of the device is 1.35 mm. G: ground; S: signal; DC: direct current

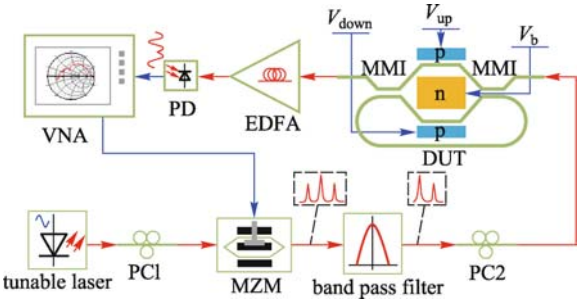

Fig. 6 Experimental setup to measure the phase shift of a RF signal induced by the device

(MZM). The modulator is driven by a single-tone RF signal from a 67-GHz vector network analyzer (VNA). The modulation generates two sidebands together with the main carrier. It then goes through a bandpass filter to get rid of the lower sideband so as to leave only the carrier and the upper sideband. The optical signal is then set to the transverse electric (TE) polarization by using another polarization controller (PC2) and coupled into the chip. The optical carrier is set at the operation wavelength of the device and will change its phase upon DC tuning. The phase of the upper sideband is kept almost constant as it is

away from the resonance. The output-coupled signal from the chip is then amplified by an erbium-doped fiber amplifier (EDFA) and detected by a photodiode (PD). The carrier and the upper sideband will beat in the PD to generate the RF signal. The RF signal was finally received by the VNA, and its amplitude and phase are compared with the initial RF signal.

From the wavelength-scanned output power spectrum, the device critical-coupling wavelength is at 1543.84 nm without bias. We first set V_b = 2.5 V to make the pn junctions work at the reverse-bias mode. The laser wavelength is tuned to the red-shifted resonance wavelength. V_{up} and V_{down} are switched between ±0.5 V to form a push-pull drive scheme. As the coupling state of the ring resonator is flipped between over-coupling and under-coupling, a π phase change is obtained at the resonance wavelength. Figure 7 shows the measured phase shift for a RF signal of various frequencies. Phase shift is stable at π except for the 5 GHz RF signal, where the carrier and the upper sideband are too close to separate by the micoring resonance. The amplitude variation between the two states is less than 1 dB.

We next generate a continuous phase change by varying the three bias voltages. The input wavelength is set to 1543.85 nm, slightly red-detuned from the initial resonance wavelength. Figure 8 shows the measured amplitude and phase changes. The RF signal frequency is 20 GHz. The tuning method follows the theoretical analysis in Section 2. A maximum of 2.5π phase shift is obtained close to the theoretical value in Fig. 3(b).

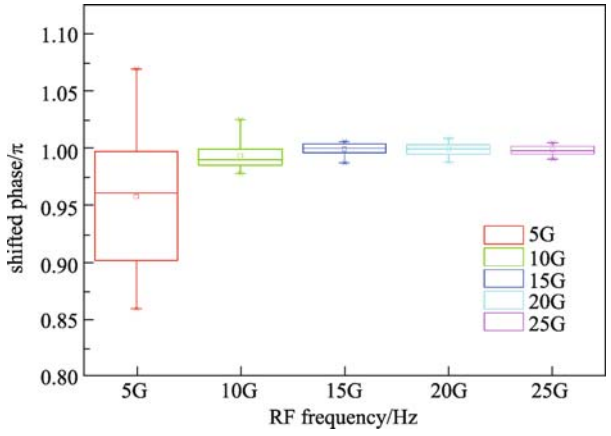

Fig. 7 Measured π phase shift for a RF signal at various frequencies

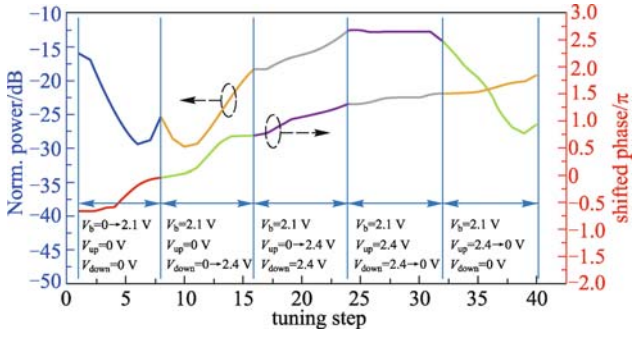

Fig. 8 Measured optical power and phase change upon bias tuning

5 Conclusions

We have reported a microwave photonic phase shifter using a coupling-modulated microring resonator. The device was first analyzed theoretically. An exact π phase change with a constant amplitude could be achieved by flipping coupling between over-coupling and under-coupling. A continuous large-range phase shift could be realized by manipulating the three bias voltages applied on the MZI coupler. The RF phase shift experiments were then carried out following the theoretical predictions. A binary π phase shift and a continuous phase change of 2.5π were obtained, agreeing well with the simulation results. The microring RF phase shifter could serve as a basic building block for compact microwave photonics signal processing and phased array radars.

Acknowledgements This work was supported in part by the National High Technology Research and Development Program (863 Program) (No. 2013AA014402), the National Natural Science Foundation of China (NSFC) (Grant Nos. 61422508), the Shanghai Rising-Star Program (No. 14QA1402600), and the Specialized Research Fund for the Doctoral Program of Higher Education (SRFDP) of Ministry of Education of China (No. 20130073130005). We also acknowledge IME Singapore for device fabrication.

References

1. Capmany J, Mora J, Gasulla I, Sancho J, Lloret J, Sales S. Microwave photonic signal processing. IEEE Journal of Lightwave Technology, 2013, 31(4): 571–586
2. Fisher M, Chuang S. A microwave photonic phase-shifter based on wavelength conversion in a DFB laser. IEEE Photonics Technology Letters, 2006, 18(16): 1714–1716
3. Loayssa A, Lahoz F J. Broad-band RF photonic phase shifter based on stimulated Brillouin scattering and single-sideband modulation. IEEE Photonics Technology Letters, 2006, 18(1): 208–210
4. Xue W, Sales S, Capmany J, Mørk J. Microwave phase shifter with controllable power response based on slow- and fast-light effects in semiconductor optical amplifiers. Optics Letters, 2009, 34(7): 929–931
5. Lee S S, Udupa A H, Erlig H, Hua Zhang, Yian Chang, Cheng Zhang, Chang D H, Bhattacharya D, Tsap B, Steier W H, Dalton L R, Fetterman H R. Demonstration of a photonically controlled RF phase shifter. IEEE Microwave and Guided Wave Letters, 1999, 9 (9): 357–359
6. Chang Q, Li Q, Zhang Z, Qiu M, Ye T, Su Y. A tunable broadband photonic RF phase shifter based on a silicon microring resonator.

IEEE Photonics Technology Letters, 2009, 21(1): 60–62
7. Pu M, Liu L, Xue W, Ding Y, Ou H, Yvind K, Hvam J M. Widely tunable microwave phase shifter based on silicon-on-insulator dual-microring resonator. Optics Express, 2010, 18(6): 6172–6182
8. Sacher W D, Poon J K. Characteristics of microring resonators with waveguide-resonator coupling modulation. IEEE Journal of Lightwave Technology, 2009, 27(17): 3800–3811
9. Yang R, Zhou L, Zhu H, Chen J. 28 Gb/s BPSK modulation in a coupling-tuned silicon microring resonator. In: Proceedings of CLEO 2015. San Jose, California, 2015, SW1N.5
10. Wang J, Qiu C, Li H, Ling W, Li L, Pang A, Sheng Z, Wu A M, Wang X, Zou S C, Gan F W. Optimization and demonstration of a large-bandwidth carrier-depletion silicon optical modulator. IEEE Journal of Lightwave Technology, 2013, 31(24): 4119–4125
11. Yariv A. Critical coupling and its control in optical waveguide-ring resonator systems. IEEE Photonics Technology Letters, 2002, 14(4): 483–485

Rui Yang received his B.S. degree in electronic information engineering from Anhui Jianzhu University, in 2012. He is currently a master student of year 3 with the State Key Laboratory of Advanced Optical Communication Systems and Networks, Department of Electronic Engineering, Shanghai Jiao Tong University. His current research interests include silicon modulators and other novel silicon based optical structures.

Linjie Zhou received his B.S. degree in microelectronics from Peking University in 2003. He received his Ph.D. degree in electronic and computer engineering from the Hong Kong University of Science and Technology in 2007. From 2007 to 2009, he worked as a postdoctoral researcher at University of California, Davis. Currently he is an associate professor in the State Key Lab of Advanced Optical Communication Systems and Networks in Shanghai Jiao Tong University. His research interests include silicon photonics, plasmonic devices and optical integration. He has been working on multiple national projects as the principle investigator, including the National Science Fund for Excellent Young Scholars. He recently has been working on large-scale optical switches, high-speed IQ modulators, and long-range tunable optical delay lines on the silicon-on-insulator platform. He has published more than 130 peer-reviewed journal and conference papers, and given more than 20 invited talks in international conferences. Dr. Zhou is a member of the Institute of Electrical and Electronic Engineers (IEEE) and the Optical Society of America (OSA).

Minjuan Wang received her B.S. degree in the Department of Optoelectronic Engineering, Nanjing University of Posts and Telecommunications (NUPT) in 2014. She is currently a graduate student with the State Key Laboratory of Advanced Optical Communication Systems and Networks, Department of Electronic Engineering, Shanghai Jiao Tong University. Her recent research interests include high-speed integrated silicon modulators and nonlinear optics.

Haike Zhu received his B.S. degree from the Physics Department, Sichuan University, in 2010. He received his Ph.D. degree in the State Key Laboratory of Advanced Optical Communication Systems and Networks in Shanghai Jiao Tong University. He is currently working at Fijikura Ltd., Japan. His research interests include high-speed integrated silicon photodetectors, and modulators.

Jianping Chen received his B.S. degree from Zhejiang University in 1983, and M. S. and Ph.D. degrees from Shanghai Jiao Tong University, Shanghai, China, in 1986 and 1992, respectively. He is currently a Professor with the State Key Laboratory of Advanced Optical Communication Systems and Networks, Department of Electronic Engineering, Shanghai Jiao Tong University. His main research interests include photonic devices and signal processing, optical networking, and sensing optics. He is also a Principal Scientist of the 973.